Article:
Blanquet, E, Nahil, MA and Williams, PT orcid.org/0000-0003-0401-9326 (2019) Enhanced hydrogen-rich gas production from waste biomass using pyrolysis with non-thermal plasma-catalysis. Catalysis Today, 337. pp. 216-224. ISSN 0920-5861

https://doi.org/10.1016/j.cattod.2019.02.033

Enhanced hydrogen-rich gas production from waste biomass using pyrolysis with non-thermal plasma-catalysis

Ella Blanquet, Mohamad A. Nahil, Paul T. Williams*

School of Chemical and Process Engineering, University of Leeds, Leeds, LS2 9JT, U.K.

(*Corresponding author; Email; p.t.williams@leeds.ac.uk; Tel; #44 1133432504)

Abstract:

A pyrolysis-non-thermal plasma-catalytic system for the increased production of hydrogen-rich gas from waste biomass has been investigated. Plasma processing of the hydrocarbon pyrolysis gases produced a marked increase in total gas yield with plasma-catalysis producing a further modest increase. The product gases were mainly composed of H_2, CO and CO_2, which were all increased under plasma and plasma-catalyst conditions. For example, H_2 yield increased from 1.0 mmol $g^{-1}_{biomass}$ in the absence of plasma to 3.5 mmol $g^{-1}_{biomass}$ with plasma and to 4.0 mmol $g^{-1}_{biomass}$ with plasma-catalysis. In addition, in the absence of plasma, the hydrocarbon tar content in the product gas was 420 mg m^{-3}, but, for non-catalytic plasma conditions, this was reduced to 325 mg m^{-3} and for plasma-catalytic steam reforming, the tar hydrocarbons were markedly reduced to 150 mg m^{-3}.

The effect of increasing input power for the plasma processing (no catalyst) showed a large increase in total gas, H_2, CO and CO_2 yield and corresponding decrease in hydrocarbon gas concentration. Plasma-catalysis showed that higher power input had only a small effect on gas yield. Plasma-catalysis was shown to produce lower catalyst coke deposition compared to non-plasma catalytic processing.

Keywords: Biomass; Gasification; Plasma; Hydrogen; Tar

1. Introduction

Climate change is described as a major global crisis resulting from human activities and has been recognised as such by several international institutions [1,2]. To tackle global warming, a combination of initiatives have been put in place: the Sustainable Energy for All from the UN [3], the COP21 "Paris agreement" signed by around 200 countries [4], as well as many local initiative such as the European Commission 2020 [5] and 2030 [6] recommendations. These initiatives emphasize the need to switch from the use of fossil fuels for energy production to the use of renewable energies and the need to improve the efficiency of energy production. Biomass has received particular interest as a renewable energy source since it can contribute to all energy sectors including electricity, heat and transport, as well as being a valuable resource for materials, products and speciality chemicals. For lignocellulosic or woody biomass, the common routes to produce fuels and energy are through combustion, pyrolysis and gasification. The production of gas from biomass is considered an attractive option since the product gas can be easily transported and stored and with potential for conversion to liquid fuels for use in transportation. [7].

Hydrogen is produced in large quantities and used in applications such as the production of ammonia, fertilisers, and methanol and is used extensively in the petroleum refining industry. There is also a predicted large increase in demand for hydrogen if the future hydrogen economy becomes a reality. Currently hydrogen is largely produced from fossil fuel natural gas, coal and petroleum oil, but there is interest in producing hydrogen from sustainable sources such as biomass [8]. The largest commercial fossil fuel route for the production of hydrogen is through the natural gas catalytic steam reforming process. Arising from this industrial experience, a novel development for the production of hydrogen from biomass involves a first stage pyrolysis of the biomass that produces a wide range of hydrocarbon gases, which are then passed to a catalytic steam reforming reactor for hydrogen production [9-12]. Thereby the process mimics the natural gas catalytic steam reforming of natural hydrocarbons, but involves a much more complex range of hydrocarbons.

A key issue in the development of hydrogen-rich gas production from biomass is the presence of the problematic higher molecular weight hydrocarbons or tar in the product gas [13]. Such problems include blocking of gas transfer lines, valves, fuel injector nozzles, etc. Tar composition includes single ring aromatic compounds such as toluene, two-ring aromatic

hydrocarbons such as naphthalene 3-5-ring and higher molecular weight polycyclic aromatic hydrocarbons (PAH) and oxygenated hydrocarbons [13, 14]. Tars have been classified based on the temperature of formation into (i) Primary Tars (~400-500 °C), consisting of mixed oxygenated hydrocarbons such as phenols, guaiacols, furfural, ketones and aldehydes (ii) Secondary Tars (~500- 800 °C) consisting of phenolic ethers, alkyl phenolic compounds and heterocyclic ethers, single ring aromatic compounds, phenols, cresol and xylenes (iii) Tertiary Tars (800 - 900 °C) PAH (2-7 ring) and more complex larger PAH [14-16]. The range of polycyclic aromatic hydrocarbons found in tars has also raised concern due to their associated carcinogenic characteristics [14]. The acceptable range for tars in higher efficiency end-use applications can be < 10 mg m^{-3} for engines, < 5 mg m^{-3} for gas turbines and < 1 mg m^{-3} for fuel cells [7]. However, tar contents of raw syngas from gasification can reach well over 10,000 mg m^{-3}, depending on the gasifier type and operational conditions [7, 17, 18].

The use of plasmas in thermochemical treatment processes related to biomass have received considerable recent interest. High temperature thermal plasma (~10,000 °C) has been used to gasify biomass to improve syngas purity and to crack tar [19]. However, there has also been recent interest in the use of non-thermal, low temperature (~200 °C) plasma to degrade tar model compound hydrocarbons [17]. Non-thermal plasma are able to generate high energy electrons (1~10 eV) which breaks the chemical bonds thereby decomposing gas phase molecules, in addition to producing chemically reactive species such as free radicals, excited atoms, ions and molecules [18, 20]. Such a highly reactive environment is conducive for the decomposition of hydrocarbon tar compounds enabling thermodynamically unfavourable reactions to occur at low temperature. The reaction has a high reaction rate and reaches rapidly steady state, without being as energetic as thermal plasma [21].

To further improve the technology, catalysts have been used in conjunction with non-thermal plasma [22, 23]. By combining both technologies, the main advantages of non-thermal plasma and catalysis technologies are combined with the aim to produce a syngas product with lower hydrocarbon tar content. In addition, synergistic effects of plasma-catalysis have been reported through interaction of the plasma and the catalyst [20, 24].

Experimental research associated with tar reduction in the field of non-thermal plasma and plasma catalysis is almost always conducted on model hydrocarbon compounds consisting of simple, single hydrocarbons [25]. For example, plasma-catalytic studies involving the reduction of toluene [25, 26-28] or naphthalene [29] as model compounds representative of

species found in tar. However, tar produced from the thermochemical processing of biomass is a very complex mixture of hydrocarbons with different physical and chemical properties.

The work presented in this paper investigates the production of a hydrogen-rich gas from biomass with reduced hydrocarbon tar content using a two-stage reactor system designed and developed specifically for the experimental programme. Pyrolysis of the biomass in the first stage reactor generated a wide range of hydrocarbon and oxygenated hydrocarbon species which were passed to the plasma/catalytic reactor in the presence of steam where plasma assisted catalytic steam reforming reactions occurred. The influence of plasma power input and steam flowrate on product gas yield and composition and also hydrocarbon tar content was investigated.

2. Materials and methods

2.1. Materials

The waste biomass used as the feedstock for pyrolysis was in the form of waste wood sawdust which was compressed into wood pellets and was obtained from Liverpool Wood Pellets Ltd, Liverpool, UK. The pellets were shredded and sieved to produce waste biomass with a particle size of 1 mm. Elemental analysis of the biomass showed a carbon content of 46.0 wt.%, hydrogen, 5.6 wt.%, nitrogen 0.7 wt.% and oxygen 45.7 wt.% (by difference). Proximate analysis of the biomass showed 75.0 wt.% volatiles 7.0 wt.% moisture 2.0 wt.% ash and 15.0 wt.% fixed carbon.

The catalyst used for the catalytic reforming and plasma-catalytic reforming of the biomass pyrolysis gases was a nickel based catalyst with an alumina (Al_2O_3) support and was prepared using an impregnation method. The catalyst was prepared as 10 wt.%Ni using $Ni(NO_3)_2.6H_2O$ which was dissolved in deionised water and the alumina support added to the mixture to produce a slurry which was heated to 60 °C. The slurry was dried and then calcined at 750 ºC with a heating rate of 2 ºC min^{-1} from ambient temperature to 750 °C. The catalyst was the crushed and sieved to a size of 1 mm. The catalyst was then reduced using a 5% hydrogen mixture in nitrogen at a temperature of 800 ºC for one hour, at a heating rate of 20 ºC min^{-1} from ambient temperature to 800 ºC. The catalyst was characterised by BET nitrogen

adsorption which gave a surface area of 155 m^2 g^{-1} and pore volume of 0.410 cm^3 g^{-1}. In addition, the fresh catalyst and the used catalysts after plasma-catalysis reaction were analysed by XRD (X-Ray Diffraction). The XRD spectra were obtained from a XRD Bruker D8 diffractometer using Mg-Kα radiation and recorded within a range of 10 to 80º using a step size of 0.25º and a counting time of 0.35 s. The XRD identification was conducted using HighScore Plus by comparing the obtained XRD patterns with the corresponding JCPDS cards.

2.2 Experimental system

The experimental system for the biomass pyrolysis-plasma-catalysis was comprised of a two stage reactor system shown in Figure 1. The first stage pyrolysis used a fixed bed, stainless steel reactor heated using a temperature controlled electric furnace. The evolved biomass pyrolysis gases were directly transferred to a second stage quartz reactor where non-thermal plasma and plasma-catalytic reforming reactions took place in the presence of steam. The use of a two-stage pyrolysis-plasma-catalysis system has advantages, in that the process conditions in each reactor stage, such as reactor temperature can be more easily controlled. In addition, the interaction of the evolved biomass pyrolysis gases and catalyst improves the contact between pyrolysis products and the catalyst and minimises mass transfer. Also, the two-stage reaction system enables the reacted catalysts to be recovered, recycled and reused. The pyrolysis and plasma-catalysis reactor were separated using an electrically insulating ceramic transfer tube. The biomass waste feedstock (1 g) was weighed into a stainless steel crucible in the pyrolysis reactor and heated to 600 ºC at a heating rate of 50 ºC min^{-1}. The 2nd stage plasma-catalysis reactor incorporated a coaxial Dielectric Barrier Discharge (DBD) plasma generated using a 80 mm long copper mesh outer electrode wrapped on a quartz tube of 25 mm o.d. and 22 mm i.d. An 18-mm stainless steel rod was used as the inner electrode placed centrally within the quartz tube. Thus the discharge region was ~80 mm with a discharge gap of 2 mm. The DBD plasma reactor was connected to an AC high-voltage power supply with a frequency of 1500 Hz and a maximum peak-to-peak voltage of 20 kV. The inner electrode was connected to the high voltage output whereas the outer electrode was grounded. A digital oscilloscope monitored the discharge. The Ni-Al_2O_3 catalyst (1 g) was placed at the centre of the discharge zone and held in place by quartz wool. The reactor system was continuously purged with nitrogen at a flow rate of 100 mL min^{-1}. The 2nd stage plasma reactor was maintained at a temperature of 250 °C using a temperature controlled electric furnace.

Steam, for the reforming of the hydrocarbon pyrolysis gases, was generated from distilled water and injected into the second stage plasma reactor. Product gases were passed through a condenser system comprised of a series of dry-ice cooled glass condensers which condensed the product liquid products and non-condensable gases were passed to a 25 L Tedlar™ gas sample bag.

The experimental procedure consisted of pre-heating the second stage plasma reactor to 250 ºC, and the pyrolysis first stage furnace to 120 ºC. The plasma was then generated and the pyrolysis of the biomass started. The evolved biomass pyrolysis gases passed into the plasma-catalysis steam reforming reactor for reaction. Once the pyrolysis reactor had reached 600 ºC, the temperature was maintained for 10 minutes during which time pyrolysis-plasma-catalysis reactions took place. The product gases were continued to be collected for a further 20 minutes to ensure all of the biomass had been pyrolysed and evolved gases reacted in the plasma-catalysis reactor. Gases were analysed later by gas chromatography to identify and quantify the product gas composition. The condensed liquid product containing both condensed hydrocarbons and water were recovered from the condensers using methanol. The recovered liquid was analysed for water content and analysis of the condensed hydrocarbon tar using coupled gas chromatography-mass spectrometry.

2.3. Gas analysis

The product gas composition was analysed by gas chromatography (GC). Using different Varian CP-3380 GCs and different packed columns, the concentrations of the permanent gases (hydrogen, carbon monoxide, nitrogen, oxygen), hydrocarbons (C_1-C_4) and carbon dioxide were determined. A Varian CP-3380 with a Restek 60-80 mesh molecular sieve column and thermal conductivity detector (TCD) was used for H_2, CO, N_2 and O_2. Due to overlapping CO and CO_2 GC peaks, a separate Varian CP-3380 GC with a Restek 80-100 mesh molecular sieve column and TCD was used for CO_2, but with different GC temperature programme conditions The hydrocarbons from C_1 to C_4 were analysed using a third Varian CP-3380 gas chromatograph, with a flame ionisation detector (GC/FID) and a 80-100 mesh HayeSep type column. The chromatographic peaks were integrated using Harley Peakmaster Integration software.

2.4. Condensed hydrocarbon tar analysis

The condensed liquid product in the condensation system was analysed for water content and hydrocarbons content. Water content was analysed by Karl Fischer Titration using a Metrohm890 Titrando apparatus and Tiamo™ 2.3 software which directly recorded the water content in the liquid product. The condensed hydrocarbons were analysed using GC/MS with a Hewlett Packard 5280 GC and a HP 5271 ion trap mass spectrometric detector. The GC column was a Restek RTX-5MS column of 30 metre length and 0.25 mm internal diameter with fused silica 95% dimethyl polysiloxane and 5% diphenyl solid phase of 25 µm film thickness. Helium was the gas carrier used. The GC/MS was calibrated with a range of aromatic and polycyclic aromatic hydrocarbons (PAH) and oxygenated hydrocarbon standards which were used as external standards for identification and quantification. In addition, the mass spectrometer was used to confirm identification. The derived ion-mass spectra were identified using the NIST 2008 spectral library to determine compound identification with an ion mass spectral similarity index of >70%. The GC/MS analysis of the hydrocarbons collected from the condensers was used to determine the influence of plasma and plasma-catalytic decomposition on total hydrocarbon tar yield and also for particular hydrocarbons indicative of tar compounds.

Size exclusion chromatography (SEC) was used to determine the molecular weight range of the condensed hydrocarbon tar. The system incorporated a 300 mm x 7.5 mm column with a Polymer Laboratories 3 µm GPC/SEC 100A type packing, which was maintained at 30 ^{o}C. Tetrahydrofuran (THF) was used as a solvent for the mobile phase with a flow rate of 1 mL min^{-1}. The calibration system used was based on polystyrene standards in the Mw range of 100-9000 Da. The detector measuring the elution of all compounds was a refractive index detector from Perkin Elmer. The output from the detector was given in millivolts and transmitted to a software, Total Chrom Navigator. The Mw distribution was determined as a molecular weight average (Mw). The samples for analysis were prepared using approximately 0.25 mL of the condensed hydrocarbon liquid with a dilution of 1/100 in the solvent, THF.

2.5. Catalyst coke analysis

The characteristics of the carbonaceous coke formed on the catalyst during reaction were determined through temperature programmed oxidation (TPO) of the catalysts. TPO oxidises the coke deposited on the catalyst in the presence of air under controlled heating rate conditions using a thermogravimetric analyser (TGA) which enables the mass of carbon

oxidised in relation to temperature to be determined. The TGA was a TGA-50 Shimadzu instrument and the oxidation temperature programme was ambient temperature to 800 °C at a heating rate of 15 °C min^{-1}.

3. Results and discussion

3.1. Plasma-catalysis for hydrogen-rich gas production

3.1.1. Comparison of catalysis, plasma and plasma-catalysis

The production of gases from the two-stage biomass pyrolysis with plasma-catalysis was investigated via comparison of two stage pyrolysis-catalysis (no plasma) and pyrolysis-plasma (no catalyst) and pyrolysis-plasma-catalysis for the steam reforming of the biomass pyrolysis gases. The experiments used a power input of 40 W to sustain the plasma discharge and an input steam flow rate of 2 g h^{-1} to simulate the steam reforming process.

The yield of gas produced in relation to pyrolysis-catalysis, pyrolysis-plasma and pyrolysis-plasma-catalysis is presented in Figure 2(a) and the detailed composition of the product gas is shown in Fig. 2(b). Pyrolysis-catalysis produced a product gas yield of 2 mmol $g^{-1}_{biomass}$. However, with the introduction of the plasma in the pyrolysis-plasma process (no catalyst) a product gas yield of ~7 mmol $g^{-1}_{biomass}$ was produced. With the introduction of the catalyst together with plasma, the consequent plasma-catalytic process produced a similar total gas yield to that for the plasma alone. In addition, the calorific value of the gases was ~12 MJ m^{-3}, for pyrolysis- catalysis, pyrolysis-plasma and pyrolysis-plasma-catalysis. However, a more detailed compositional analysis of the produced gas shows that the individual gas yields were changed in the presence of the plasma-catalytic steam reforming system compared to plasma alone (Fig. 2(b)). Decreased CH_4 yields in the presence of plasma and plasma-catalysis suggests steam reforming of the CH_4, but also the higher molecular weight hydrocarbon gases, which produced an increased yield of H_2 (Eq. 1). The plasma-catalytic process produced increased H_2 and CO_2 and reduced CO yields, which suggests that the catalyst promotes not only the steam reforming of the pyrolysis hydrocarbons but also the water gas shift reaction (Eq. 1, Eq. 2) [30]. The nickel catalyst is a known material for breaking down tar compounds in gasification processes, by steam reforming leading to a higher hydrogen gas production [31].

In plasma-catalysis, compared to the plasma process, the higher H_2 production was most likely the result of reduction of tar hydrocarbons by the Ni-catalyst.

$$C_nH_m + nH_2O \rightarrow nCO + (n + m/2)H_2 \quad \text{(Eq. 1)}$$

$$CO + H_2O \rightarrow CO_2 + H_2 \quad \text{(Eq. 2)}$$

The reaction of CO_2 to produce excited CO^* and O_2^*species, has been reported to take place in plasma reaction zones [32, 33], the recombination of the excited O_2^* species, is likely to lead to oxygen production which was observed in the product gases for the plasma and plasma-catalytic systems. Considering the slight increase of oxygen in the plasma system, where the carbon monoxide concentration was the highest, the combination of both reactions could explain the differences between the plasma and plasma-catalytic system.

It is important to note that the Ni-Al_2O_3 catalyst is typically used for high temperature steam reforming at temperatures of ~ 800 °C [34] and not low temperature plasma-catalysis at temperatures of ~250 °C. Therefore, the catalyst may have low catalytic activity at the operating temperature used in this work. However, it has been reported that the water gas-shift reaction can occur at temperatures of 200-300 ºC [35, 36]. The temperature inside the second stage plasma reactor was maintained at 250 ºC, but temperature inside the plasma reactor zone may be higher than this, also the Ni-Al_2O_3 catalyst may show some activity, particularly if the plasma promotes surface catalytic reactions.

3.1.2. Influence of process parameters

The influence of increasing power input to the plasma system was investigated to determine the influence on product gas yield and gas composition at input powers of 40, 60 and 80 W. A steam flow of 2 g h^{-1} was used throughout the experiments. The results in relation to product gas yield at increasing power input for plasma and plasma-catalytic systems are presented in Figure 3(a). For both plasma and plasma-catalysis the increase of power input led to an increase of product gas yield.

The detailed composition of the produced gas are shown in Figure 3(b) for the pyrolysis-plasma process and in Figure 3(c) for the pyrolysis-plasma-catalysis process. For each input power, more hydrogen was produced with the plasma-catalytic process compared

to the plasma only process. For example, 3.5 mmol H_2 $g^{-1}_{biomass}$ feedstock was produced for the plasma system at 40W and 4.0 mmol H_2 $g^{-1}_{biomass}$ feedstock for the plasma-catalytic system. On the other hand, carbon monoxide production was higher for the plasma system compared to plasma-catalysis for each power input. Methane production for both systems and all powers were very similar, at around 1 mmol $g^{-1}_{biomass}$. The influence of increasing plasma power input on the calorific value of the product gases was negligible, being between 11.8 - 12.2. MJ m^{-3}.

To study the effect of steam flow rate on the plasma-catalysis system for product gas yield, the plasma-catalytic system was investigated at a power input of 40W. These experiments were conducted for different steam (water) flow rates, from 0 to 6 g h^{-1}. The results are shown in Figure 4(a) for the total product gas produced and 4(b) for the detailed gas composition. The production of gas was highest at 2 g h^{-1} steam flow rate as shown in Fig. 4(a). The absence of steam produced lowered gas production and hydrogen production (Fig. 4(b)). Without steam, the number of active $OH^{\bullet}$ radicals would be reduced and thus could not participate in the collisions and creation of active species leading to H_2 production. Water is a product of biomass pyrolysis, therefore it would be expected that $OH^{\bullet}$ radicals would be generated in the plasma zone, but the amount would be reduced in relation to additional steam input. At higher steam flows, the catalyst partially lost its activity and efficiency, the optimum steam flow in terms of the production of product gas was 2 g h^{-1}.

3.2. Plasma-catalysis for hydrocarbon tar reduction

3.2.1. Comparison of catalysis, plasma and plasma-catalysis

The two-stage biomass pyrolysis with plasma-catalysis was also used to investigate the effect of plasma and plasma-catalysis on the steam reforming process for the reduction of the higher molecular weight hydrocarbon tar species. Fig. 5(a) shows the total hydrocarbon tar content of the product gas in relation to the pyrolysis-catalysis, pyrolysis-plasma and pyrolysis-plasma-catalysis systems for the steam reforming of the biomass pyrolysis tars. The total hydrocarbon tar content was determined from the analysis of the total hydrocarbons condensed in the reactor condensation system and detected using the GC/MS analytical system. The results were then converted to mg tar m^{-3} of gas based on the total gas throughput. Fig. 5(b) shows the detailed analysis of the tars for selected tar hydrocarbons in relation to process conditions. The selected hydrocarbons represented the range of molecular weights found in light tars with molecular weights from benzene (M.Wt.78) to higher molecular weight

compounds with molecular weights over 160 MW units. The selected hydrocarbons were, alkylated-phenols or aromatic compounds: benzene, phenol, o-cresol, p/m-cresol, guiaicol, 2,4-dimethylphenol, 4-ethylphenol, 4-isopropylphenol and 2-methoxy-4-propylphenol. The product gas total tar content was 420 mg m^{-3} for the pyrolysis-catalysis system, but was reduced to 335 mg m^{-3} for the pyrolysis-plasma system. However, with the introduction of the catalyst into the plasma zone, the hydrocarbon tar content in the product gas was markedly reduced to 150 mg m^{-3}. Compared to the hydrocarbon tar content in the absence of the plasma (pyrolysis-catalysis) the pyrolysis-plasma system represents a reduction in hydrocarbon tar content of 21% and 64% reduction for the pyrolysis-plasma-catalysis system.

The detailed comparison of the selected hydrocarbons in the hydrocarbon tar in the product syngas shown in Fig. 5(b) shows that the individual aromatic and oxygenated aromatic hydrocarbons are reduced in concentration in the plasma and plasma-catalytic processes. The plasma-catalytic process producing the highest reduction in concentration of the selected hydrocarbons. In addition, the larger hydrocarbon tar molecules with very high boiling points will also be reduced in concentration. Figure 6 shows the average molecular weight and the molecular weight range of the condensed hydrocarbons determined using size exclusion chromatography in relation to the influence of plasma on the process. Figure 6(a) shows that the pyrolysis hydrocarbons had a very wide molecular weight range from ~100 to over 1000 Mw units. The introduction of the Ni-Al_2O_3 catalyst to the system produced a marked decrease in the molecular weight range of the hydrocarbon tars, as was also shown by the pyrolysis-plasma process. However, the pyrolysis-plasma-catalysis process showed that the product hydrocarbon tars were reduced to produce a low molecular weight range tar. Figure 6(b) for the average molecular weight of the hydrocarbon tars shows that the pyrolysis only system produced the highest average molecular weight of 885 Mw compared to pyrolysis-catalysis at 169 average Mw and pyrolysis-plasma at 126 average Mw systems. The lowest average molecular weight was obtained for the pyrolysis-plasma-catalysis system (102 Mw). The marked decrease in average molecular weight showing that the post-pyrolysis processing of the biomass pyrolysis gases using catalyst, plasma or plasma-catalysis produces a major decrease in the high molecular weight hydrocarbon tar content of the product gas. Such high molecular weight hydrocarbon tars are the problematic tar species that are the main cause of blockages of gas fuel transfer lines, fuel injectors, etc.

In the plasma process, the plasma produces high energy electrons which activate the reactants initiating radical reactions [17]. The reduction in tar yield for the plasma and plasma-

catalytic systems may be attributed to the reactive plasma species including high energy electrons, the free radicals such as $OH^{\bullet}$, $O^{\bullet}$ and $N^{\bullet}$ and excited N_2^* species reacting with the biomass pyrolysis products [25]. These short-life species can breakdown the tar compounds through collision, generating smaller molecular weight species [37].

The marked reduction in hydrocarbon tar content in the product gas from the plasma-catalytic process involves the interaction of the plasma with the catalyst enhancing tar reduction reactions. The presence of the catalyst particles in the discharge gap will enhance charge accumulation on the particle surface, resulting in increased local or average electrical field and thereby the number of high energy electrons and reactive species [38]. In addition to this physical effect of the particles, the presence of electrically conductive nickel particles on the catalyst surface will also increase the plasma development and provide nickel metal sites for the catalysed decomposition of the biomass thermal degradation species. The plasma-catalysis system enables plasma generated, high energy electrons, ions, radicals and excited species to interact with the catalyst, which will not be the case for thermal catalysis [24]. The presence of the catalyst within the plasma zone enables both plasma induced reactions and also catalytically promoted reactions to occur. The plasma will activate the pyrolysis gases to produce a complex mixture of molecules, free radicals, excited species, atoms, ions and electrons which will both interact in the gas phase and on the catalyst surface [24]. In addition, the catalyst surface characteristics, metal species content and dielectric properties will modify the plasma properties on the catalyst, enhancing decomposition of the pyrolysis products. The presence of the plasma may also alter the physicochemical properties of the catalyst surface. It should also be noted that the presence of the packing material particles of the Al_2O_3 support may have dielectric properties which act as a physical effect on the plasma-solid interaction which induces the chemical effects that enhances pyrolysis product degradation. This effect is in addition to the presence of the active nickel species present in the catalyst which enhances selective reforming and cracking reactions. The pore size distribution of the catalyst will also influence pyrolysis product decomposition where it has been reported that strong electric fields are produced due to micro-discharges in the catalyst pore volume [24].

Comparison of the hydrocarbon tar reduction results from biomass may be compared to model compound work reported in the literature. For example, Liu et al. [25] used a dielectric barrier discharge system to study the non-thermal plasma-catalytic steam reforming of toluene as a tar model compound using a range of different catalysts. The catalysts used were Ni and Fe based catalysts with different support materials. They reported that the Ni catalysts were

more effective in converting the toluene to product gas and that the surface area of the support influenced toluene decomposition, with higher surface area support material increasing decomposition. They also investigated the location of the catalysts in the reactor system and showed that placing catalyst within the plasma zone was more effective for toluene decomposition. This was attributed to the reactive plasma species including the radicals $OH^{\bullet}$, $O^{\bullet}$ and $N^{\bullet}$ and excited species N_2^* reacting with the toluene on the surface of the catalyst. A maximum toluene conversion of 86.5% was achieved with the Ni-ZSM-5 catalyst, whereas in the absence of catalyst the conversion efficiency for the plasma only system was ~64%. Liu et al. [38] also used a dielectric barrier discharge system and a Ni-Al_2O_3 catalyst to study the catalytic steam reforming of toluene as a model biomass gasification tar compound. They investigated the influence of different Ni catalyst contents on toluene decomposition. In the absence of catalyst, the toluene conversion was 39.5% but when the Ni-catalyst was added, conversion of toluene was increased and at the highest catalyst Ni content of 20 wt.% conversion reached 51.9%. The main product gases were H_2, CO_2 and CH_4 and lower concentrations of $C_1 - C_4$ hydrocarbons. In addition, the condensed hydrocarbons from the toluene decomposition in the absence of a catalyst (plasma only) produced a range of aromatic and oxygenated hydrocarbons which were significantly reduced in the plasma-catalytic process. Benzene and ethylbenzene were identified as reaction products from the plasma-catalytic reforming of toluene, but a wide range of other hydrocarbons were also detected, including xylenes, styrene, propylbenzene and oxygenated hydrocarbons [25].

The biomass pyrolysis products generated in the first stage pyrolysis process and passed to the plasma-catalytic system are highly complex and therefore the degradation mechanism is difficult to develop. Even simple single tar model compounds have been shown to generate a range of hydrocarbon and oxygenated hydrocarbon products. For example, Wang et al [39] used a dielectric barrier discharge (DBD) plasma-catalytic reactor with CeO_2-MnO_x catalysts to study the decomposition of toluene. They identified, a range of aliphatic and aromatic hydrocarbons in the degradation products, including methyl- and diemethylbenzenes, benzaldehyde and methylbutanol. Liu et al [25] also used a DBD reactor to investigate the plasma-catalytic decomposition of toluene, using different Ni-based and Fe-based catalysts on different catalyst supports. They reported that benzene and ethylbenzene were the main products of toluene decomposition with lower concentrations of xylene, styrene, cumene, propylbenzene, isobutlybenzene, 1,2-diphenylethane and 2-methyl-3-phenylbutane. Therefore, the biomass pyrolysis gases will undergo extensive reaction and decomposition in the plasma-

catalytic system generating a wide range of hydrocarbon species as reflected in the molecular weight range of the hydrocarbon tars shown in Figure 6.

Temperature programmed oxidation was used to determine the amount of carbonaceous coke deposited on the catalysts for the pyrolysis-catalysis process and the pyrolysis-plasma-catalysis process. The pyrolysis-catalysis process resulted in a coke deposition of 10.2 wt.% compared to the coke deposition with the pyrolysis-plasma-catalysis process where coke deposition was significantly lower at 7.7 wt.%. The TPO thermograms showed that oxidation of the catalyst carbon was complete at an oxidation temperatures below 550°C. It has been reported that TPO analysis of catalyst carbon deposits can be used to distinguish between different types of carbon deposits; amorphous carbons which are oxidised at lower temperatures (<550 °C) and more graphitic filamentous carbons which oxidise at higher temperatures (>550 °C) [40]. Therefore, the data indicates that the carbon deposited on the catalyst surface was mostly amorphous carbon. During plasma-catalysis the catalyst environment is at a higher temperature than for catalysts alone [41]. This has been suggested to be due to the excited molecules colliding with energetic electrons and leading to a slight temperature increase by energy transfer between the electrons and the heavy molecules [41]. The higher plasma-induced catalyst temperature leading to increased carbon reaction and thereby reduced catalyst coke formation. It has also been suggested that the contribution of the Boudouard reaction to plasma-catalysis leads to lower catalyst coke formation compared to catalysis alone [42].

3.2.2. Influence of process parameters

The influence of plasma discharge power in relation to hydrocarbon tar reduction was investigated for the plasma and plasma catalytic systems, different powers were studied, 40, 60 and 80 W. A steam flow of 2 g h^{-1} was also used to simulate the reforming process. The results are shown in Fig. 7. The plasma-catalysis produced less hydrocarbon tar than the plasma alone process at all the power inputs investigated. The hydrocarbon tar content in the plasma system was approximately twice the hydrocarbon tar content in the plasma-catalytic system. Moreover, the higher the input power, the lower the product gas hydrocarbon tar content. The optimum result obtained was <135 mg m^{-3} product gas hydrocarbon tar content for a plasma-catalytic system with an input power of 80 W which produced a hydrocarbon tar reduction of 68% compared to the hydrocarbon tar produced with the pyrolysis-catalysis process. The evolution

of hydrocarbon tar content and increased gas production may be attributed to an increase of electric field, electron temperature as well as the temperature of the discharge gas as the input power is increased. Thus more energetic electrons and active species are created, leading to an easier breakdown of molecules. This has been observed in the conversion of carbon dioxide in atmospheric DBD by Paulussen et al. [43].

The influence of input steam flow rate to the pyrolysis-plasma-catalytic process was investigated at 0, 2, 4 and 6 g h^{-1} steam (water) input for a fixed power input of 40 W. The results are shown in Figure 8. At zero steam input the hydrocarbon tar content of the product gas was 195 mg m^{-3}, but as steam was introduced, the hydrocarbon tar content was reduced due to an increase in steam reforming reactions, decreasing to 150 mg m^{-3} at 2 g h^{-1} steam input and further reducing to 125 mg m^{-3} at 4 g h^{-1} steam input. Input of steam results in higher hydroxyl radical production generated by the radiolysis of water leading to reduction in hydrocarbon tar [44, 45]. Nunnally et al. [46] have also emphasised the importance of plasma $OH^{\bullet}$ radical production in the steam reforming process. The $OH^{\bullet}$ formed either through electron interaction with H_2O or with electrically excited interaction of O_2^* and N_2^* with H_2O. The produced $OH^{\bullet}$ radicals readily react with the hydrocarbon tar compounds resulting in decomposition. However, at higher steam input hydrocarbon tar content increased to 170 mg m^{-3}, suggesting a lowering of the hydrocarbon tar reduction efficiency of the process. Chun et al [44] have also reported that at higher steam inputs the efficiency of benzene removal decreased due to the electronegative characteristics of water. High steam input generates a high number of water molecules which limit the electron density in the system and quenches the activated chemical species. Also, in experiments conducted by Van Durme et al [27] on toluene removal in humid air by a plasma-catalytic system, water formed mono or multi-layers on the catalyst surface, preventing access to the catalyst active sites.

Temperature programmed oxidation analysis of the used catalysts in relation to plasma-catalysis at different steam inputs showed that the carbonaceous coke deposits on the catalyst at zero steam input produced a coke deposit of 11.0 wt.% However, with the addition of steam at high water flow rates, the coke deposition was reduced to 6.0 wt.% at 4 g h^{-1} steam input due to steam and CO_2 gasification reactions of the deposited carbon.

The fresh nickel supported alumina catalyst and the used catalysts after reaction were characterised by X-ray diffraction (XRD). Figure 9(a) shows the XRD spectra for the fresh prepared Ni-Al_2O_3 catalyst, the Ni-Al_2O_3 catalyst after reduction and the catalyst after reaction in the plasma-catalytic system. The XRD spectra shows that three diffraction peaks were

observed around the most intense peaks of NiO-Al_2O_3: 2θ at 37.3°, 43.3° and 62.9° (JCPDS 78-0643). The diffraction peaks for the fresh catalyst were more intense than for the reduced fresh catalyst. This suggests that smaller nickel particles are produced after reduction [47]. After reduction, a new XRD peak around 51° could be observed, which matched one of the most intense peaks of Ni: 2θ at 44.5°, 51.8° and 76.4° (JCPDS 65-2865). The diffraction spectra for the catalyst after reaction in the plasma-catalytic system were less intense compared with the peaks for the unreacted catalysts. This suggests that the nickel particles were smaller after processing in the plasma-catalytic system.

The used Ni-Al_2O_3 catalysts after use in the plasma-catalytic system with different power inputs were also analysed by XRD and the resultant XRD spectra are shown in Figure 9(b). For the catalysts with a power input of 40 W, 60 W and 80 W, the diffraction peaks were more intense for a reaction with a power input of 60 W, with lower peak intensities found at power inputs of 40 W and 80 W. This relates to the nickel particle size suggesting a smaller nickel particle size for the catalysts used at 80 W input power, followed by 40 W and 60 W. It has been suggested that the rate of carbon formation increases with the particle size [48, 49]. Thus, the formation of carbon is less likely to occur with a power input of 80 W, confirmed by the results obtained with TPO analysis used to determine the carbon deposition on the used catalysts.

4. Conclusions

The plasma-catalysis process has been investigated for the production of hydrogen-rich gas using real-world biomass as the feedstock. The process involves initial pyrolysis of the biomass to generate a wide range of hydrocarbon gases which are then passed directly to the plasma-catalysis steam reforming reactor. The influence of plasma alone and various process parameters were investigated. The results showed that plasma processing of the biomass pyrolysis gases in the absence of a catalyst resulted in a marked increase in total gas yield, including a three-fold increase in hydrogen, compared with catalytic steam reforming without plasma. Addition of catalyst (plasma-catalysis) produced a similar total product gas yield, but the hydrogen yield was further increased.

A wide range of aromatic and oxygenated compounds were identified in the condensed hydrocarbon tar phase. Pyrolysis-catalysis (non-plasma) processing was shown to reduce the yield of tar but the introduction of non-thermal plasma to the process produced a decrease in

tar content of the product gas by a further 64%. Even plasma alone (biomass pyrolysis-plasma) was found to be more efficient to remove tar from the product gas, with a 21% reduction in tar content compared to pyrolysis-catalysis. The reforming of the hydrocarbon tar compounds producing increased hydrogen content of the product gas.

The influence of power input to the plasma system showed that increasing the power markedly increased total gas yield and also hydrogen content of the product gas. There was a corresponding decrease in the tar produced for the pyrolysis-plasma system and also a further slight tar reduction for the pyrolysis-plasma-catalytic system. The influence of the steam flowrate on the system showed that there was an optimum input rate of steam. At high steam inputs, the catalyst became saturated with water resulting in the plasma-catalytic process becoming less efficient resulting in a decrease in total gas and hydrogen production and consequent rise in tar content of the product gas.

Acknowledgements

The authors gratefully acknowledge the support of the UK Engineering and Physical Sciences Research Council (EPSRC) for funding in support of the research, through EPSRC Grants EP/M013162/1 and EP/L014912/1.

References

[1]. IPCC. Summary for Policymakers. Climate Change 2014: Synthesis Report. Contribution of Working Groups I, II and III to the Fifth Assessment Report of the Intergovernmental Panel on Climate Change, 2014. doi:10.1017/CBO9781107415324

[2]. S. Teske, G.S. Sawyer, Energy [R]evolution - A Sustainable World Energy Outlook. Greenpeace International, Amsterdam, 2015.

[3]. The World Bank & IEG. World Bank Group Support to Electricity Access, FY2000-2014. World Bank Group, Washington, 2014.

[4]. European Commission. Paris Agreement Climate Action. European Commission, Brussels, 2017. Available at: https://ec.europa.eu/clima/policies/international/negotiations/paris_en.

[5]. European Commission. 2020 Energy Strategy - European Commission. European Commission, Brussels. 2017. Available at: https://ec.europa.eu/energy/en/topics/energy-strategy-and-energy-union/2020-energy-strategy.

[6]. European Commission. 2030 Energy Strategy - European Commission. European Commision, Brussels, 2017. Available at: https://ec.europa.eu/energy/en/topics/energy-strategy-and-energy-union/2030-energy-strategy. 2017.

[7]. S. K. Sansaniwal, K. Pal, M. A. Rosen, S. K. Tyagi, Recent advances in the development of biomass gasification technology: A comprehensive review. Renew. Sus. Energy Rev. 72 (2017) 363-384.

[8]. H. Balat, E. Kırtay, Hydrogen from biomass–present scenario and future prospects. Int. J. Hydrogen Energy, 35 (2010) 7416-7426.

[9]. Q.M.K. Waheed, P.T. Williams, Hydrogen production from high temperature pyrolysis/steam reforming of waste biomass: rice husk, sugar cane bagasse, and wheat straw., Energy Fuel. 27 (2013) 6695-6704.

[10]. L. Dong, C. Wu, H. Ling, J. Shi, P.T. Williams, J. Huang, Promoting hydrogen production and minimizing catalyst deactivation from the pyrolysis-catalytic steam reforming of biomass on nanosized NiZnAlOx catalysts. Fuel 188 (2017) 610-620.

[11]. C. Wu, P.T. Williams, Hydrogen production from biomass gasification with Ni/MCM-41 catalysts: Influence of Ni content. Appl. Catal. B: Environ. 108 (2011) 6-13.

[12]. C.E. Efica, C. Wu, P.T. Williams, Syngas production from pyrolysis-catalytic steam reforming of waste biomass in a continuous screw kiln reactor. J. Anal. Appl. Pyrolysis 95 (2012) 87-94.

[13]. Z. A. El-Rub, E. A. Bramer, G. Brem, Review of catalysts for tar elimination in biomass gasification processes. Ind. Eng. Chem. Res. 43 (2004) 6911-6919.

[14]. G. Guan, M. Kaewpanha, X. Hao, A. Abdula, Catalytic steam reforming of biomass tar: prospects and challenges. Renew. Sus. Energy Rev. 58 (2016) 450-461.

[15]. P. H. Blanco, C. Wu, J. A. Onwudili, P. T. Williams. Characterisation of tar from the pyrolysis/gasification of refuse derived fuel: Influence of process parameters and catalysis. Energy Fuel. 26 (2012) 2107-2115.

[16]. T. Milne, R. J. Evans, N. Abatzoglou, Biomass Gasifier 'Tars': Their Nature , Formation , and Conversion. NREL/TP-570-25357, NREL, Golden Colorado, 1998.

[17]. K. Tao, N. Ohta, G. Liu, Y. Yoneyama, T. Wang, N. Tsubaki, Plasma enhanced catalytic reforming of biomass tar model compound to syngas. Fuel 104 (2013) 53-57.

[18]. S. A. Nair, A. J. M. Pemen, K. Yan, E. J. M. van Heesch, K. J. Ptasinski, A. A. H. Drinkenburg, Chemical processes in tar removal from biomass derived fuel gas by pulsed coronoa discharges. Plasma Chem. Plasma P. 23 (2003) 665-680.

[19]. F. Fabry, C. Rehmet, V. Rohani, L. Fulcheri, Waste gasification by thermal plasma: A review. Waste Biomass Valori. 4 (2013) 421–439.

[20]. D. H. Mei, B. Ashford, Y. L. He, X. Tu, Plasma-catalytic reforming of biogas over supported Ni catalysts in a dielectric barrier discharge reactor: Effect of catalyst supports. Plasma Process. Polym. 14 (2017) 1-13.

[21]. C. Tendero, C. Tixier, P. Tristant, J. Desmaison, P. Leprince, Atmospheric pressure plasmas: A review. Spectrochim. Acta B 61 (2006) 2–30.

[22]. H. L. Chen, H. M. Lee, S. H. Chen, M. B. Meng, S. J. Yu, S. N. Li, Removal of volatile organic compounds by single-stage and two-stage plasma catalysis systems: A review of the performance enhancement mechanisms, current status, and suitable applications. Environ. Sci. Technol. 43 (2009) 2216–2227.

[23]. H. H. Kim, Y. Teramoto, A. Ogata, H. Takagi, T. Nanba, Plasma catalysis for environmental treatment and energy applications. Plasma Chem. Plasma P. 36 (2016) 45–72.

[24]. E. C. Neyts, A. Bogaerts, Understanding plasma catalysis through modelling and simulation-A review. J. Phys. D: Appl. Phys. 47 (2014) 224010 (18pp).

[25]. L. Liu, Q. Wang, J. Song, S. Ahmad, X. Yang, Y. Sun, Plasma-assisted catalytic reforming of toluene to hydrogen rich syngas. Catal. Sci. Technol. 7 (2017) 4216-4231.

[26]. S. M. Oh, H. H. Kim, H. Einaga, A. Ogata, S. Futamura, D. W. Park, Understanding plasma catalysis through modelling and simulation - A review. Thin Solid Films 506-507 (2006) 418–422.

[27]. J. van Durme, J. Dewulf, W. Sysmans, C. Leys, H. van Langenhove, Efficient toluene abatement in indoor air by a plasma catalytic hybrid system. Appl. Catal. B: Environ.

74 (2007) 161–169.

[28]. A. M. Harling, H. Kim, S. Futamura, J. C. Whitehead, Temperature dependence of plasma - datalysis using a nonthermal, atmospheric pressure packed bed; the destruction of benzene and toluene. J. Phys. Chem. 111 (2007) 5090–5095.

[29]. M. H. Yuan, C. C. Chang, C. Y. Chang, Y. Y. Lin, J. L. Shie, C. H. Wu, J. Y. Tseng, D. R. Ji, Radio-frequency-powered atmospheric pressure plasma jet for the destruction of binary mixture of naphthalene and n-butanol with Pt/Al_2O_3 catalyst. J. Taiwan Inst. Chem. Eng. 45 (2014) 468–474.

[30]. A. Kumar, A Sharma, P. Bhandari, P. Biomass gasification and syngas utilization. In Sustainable Bioenergy Production pp341-360, 2014. doi:10.1201/b16764-21

[31]. R. Zhang, R. C. Brown, A. Suby, K. Cummer, Catalytic destruction of tar in biomass derived producer gas. Energy Convers. Manag. 45 (2004) 995–1014.

[32]. S.L. Brock, T. Shimohjo, M. Marquez, C. Marun, S. L. Suib, H. Matsumoto, Y. Hayashi, Factors Influencing the decomposition of CO_2 in AC fan-type plasma reactors: Frequency, waveform, and concentration effects. J. Catal. 184 (1999) 123–133.

[33]. G. Zheng, J. Jiang, Y. Wu, R. Zhang, H. Hou, The Mutual Conversion of CO_2 and CO in Dielectric Barrier Discharge (DBD). Plasma Chem. Plasma P. 23 (2003) 59–68.

[34]. S. Czernik, R. French, C. Feik, E. Chornet, Biomass Thermoconversion Processes. Ind. Eng. Chem. Res .41 (2002) 4209–4215.

[35]. S. Hilaire, X. Wang, T. Luo, R. J. Gorte, J. A. Wagner, A comparative study of water-gas-shift reaction over ceria-supported metallic catalysts. Appl. Catal. A: Gen. 258 (2004) 271–276.

[36]. B.A. Smith, Review of the water gas shift reaction kinetics. Int. J. Chem. React. Eng. 8 (2010) 1–32.

[37]. B. Eliasson, U. Kogelschatz, Nonequilibrium volume plasma chemical processing. IEEE Trans. Plasma Sci. 19 (1991) 1063–1077.

[38]. S. Y. Liu, D. H. Mei, M. A. Nahil, S. Gadkani, S. Gu, P.T. Williams, Hybrid plasma-catalytic steam reforming of toluene as a biomass tar model compound over Ni/Al_2O_3 catalysts. Fuel Proc. Technol. 166 (2017) 269-275.

[39]. B. Wang, C. Wei, Meng Xu, C. Wang, D. Meng, Plasma-catalytic removal of toluene over CeO_2-MnO_x catalysts in an atmospheric dielectric barrier discharge. Chem. Eng. J. 322 (2017) 679-693

[40]. D. Yao, C. Wu, H. Yang, Q. Hu, M. A. Nahil, H. Chen, P.T. Williams, Hydrogen production from catalytic reforming of the aqueous fraction of pyrolysis bio-oil with modified Ni-Al catalysts. Int. J. Hydrogen Energy 39 (2014) 14642–14652.

[41]. A. Fridman, Plasma Chemistry. Cambridge University Press, 2008.

[42]. S. Kameshima, K. Tamura, Y. Ishibashi, T. Nozaki, Pulsed dry methane reforming in plasma-enhanced catalytic reaction. Catal. Today 256 (2015) 67–75.

[43]. S. Paulussen, B. Verheyde, X. Tu, C. de Bie, T. Martens, D. Petrovic, A. Bogaerts, B. Sels, Conversion of carbon dioxide to value-added chemicals in atmospheric pressure dielectric barrier discharges. Plasma Sources Sci. Technol. 19 (2010) 034015 (6pp).

[44]. Y. N. Chun, S. C. Kim, K. Yoshikawa, Decomposition of benzene as a surrogate tar in a gliding arc plasma. ,Environ. Prog. Sus. Energy 32 (2013) 837-845.

[45]. M. S. Lim, Y. N. Chun, Light tar decomposition of product pyrolysis gas from sewage sludge in a gliding arc plasma reformer. Environ. Eng. Res. 17 (2012) 89-94.

[46]. T. Nunnally, A. Tsangaris, A. Rabinovich, G. Nirenberg, I. Chernets, A. Fridman, Gliding arc plasma oxidative steam reforming of a simulated syngas containing naphthalene and toluene. Int. J. Hydrogen Energy 39 (2014) 11976-11989.

[47]. X. Yan, Y. Liu, B. Zhao, Z. Wang, Y. Wang, C.J. Liu, Methanation over Ni/SiO2: Effect of the catalyst preparation methodologies. Int. J. Hydrogen Energy 38 (2013) 2283–2291.

[48]. D. Chen, K.O. Christensen, E. Ochoa-Fernández, Z. Yu, B. Tøtdal, N. Latorre, A. Monzón, A. Holmen, Synthesis of carbon nanofibers: Effects of Ni crystal size during methane decomposition. J. Catal. 229 (2005) 82–96.

[49]. K.O. Christensen, D. Chen, R. Lødeng, A. Holmen, A. Effect of supports and Ni crystal size on carbon formation and sintering during steam methane reforming. Appl. Catal A: Gen. 314 (2006) 9–22.

Figure Captions

Fig 1. Schematic diagram of the experimental pyrolysis-plasma-catalytic reactor system

Fig.2. Comparison of 2(a) total syngas production and 2(b) detailed gas composition for catalysis, plasma and plasma-catalysis processes

Fig.3. Comparison of 3(a) total syngas production and 3(b) detailed gas composition for plasma and 3(c) plasma-catalysis of biomass pyrolysis gases in relation to plasma input power

Fig. 4. Effect of steam flow on 4(a) syngas production and 4(b) detailed gas composition at 40 W input power for the pyrolysis-plasma-catalysis of biomass

Fig. 5. Comparison of tar content 5(a) and composition of selected hydrocarbon tar compounds 5(b) for catalyst, plasma and plasma-catalysis of biomass pyrolysis gases.

Fig. 6. Molecular weight range (6(a)) and the weight average molecular weight (6(b)) of the product condensed hydrocarbon tars.

Fig. 7. Product gas tar content in relation to plasma input power for catalyst, plasma and plasma-catalysis of biomass pyrolysis gases

Fig. 8. Product gas tar content in relation to steam (water) input flowrate in relation to tar content for the plasma-catalysis of biomass pyrolysis gases

Fig. 9. XRD spectra of 9(a) the fresh, reduced and used plasma-catalysts and 9(b) the used plasma-catalysts in relation to power input

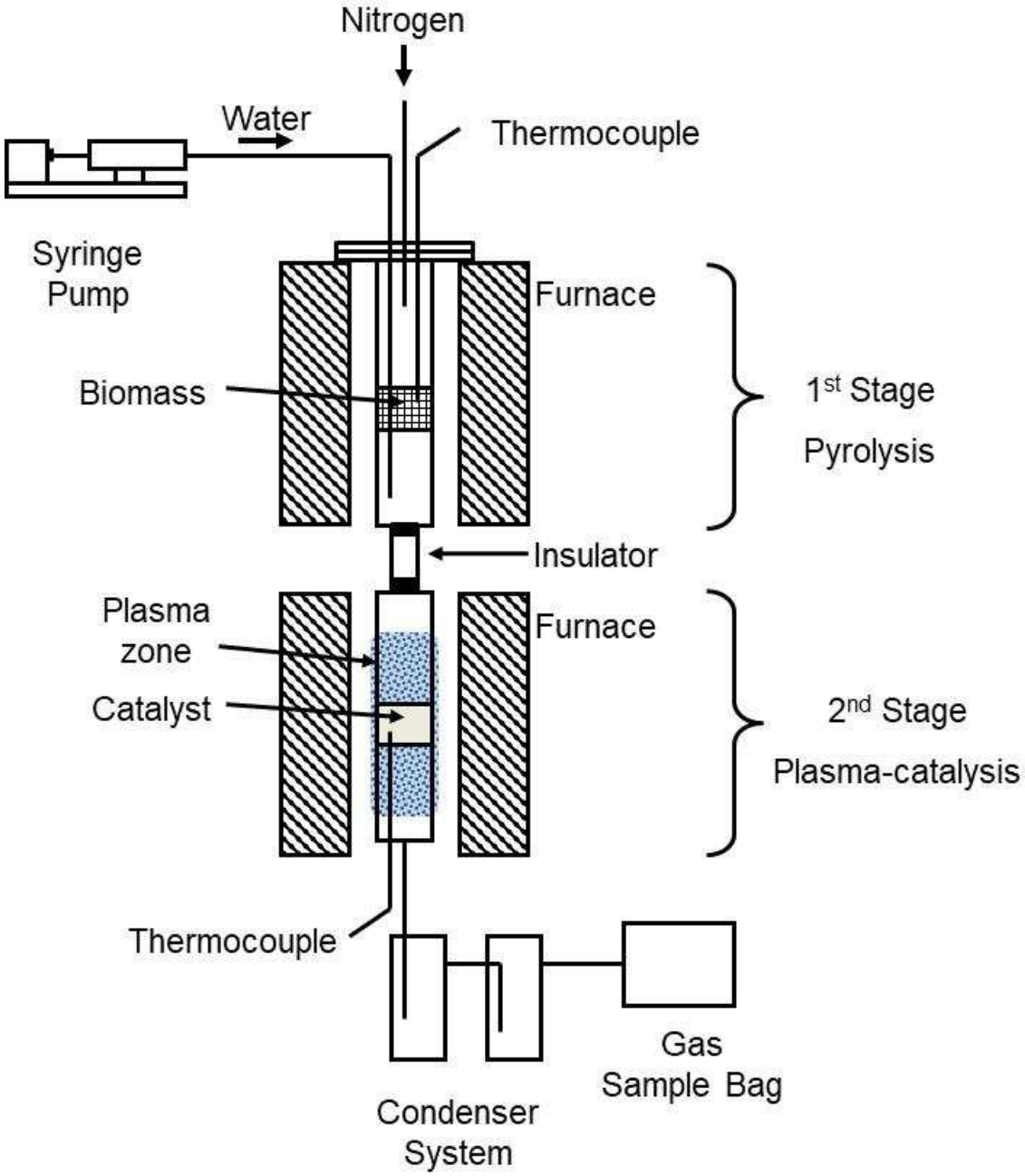

Fig 1. Schematic diagram of the experimental pyrolysis-plasma-catalytic reactor system

(a)

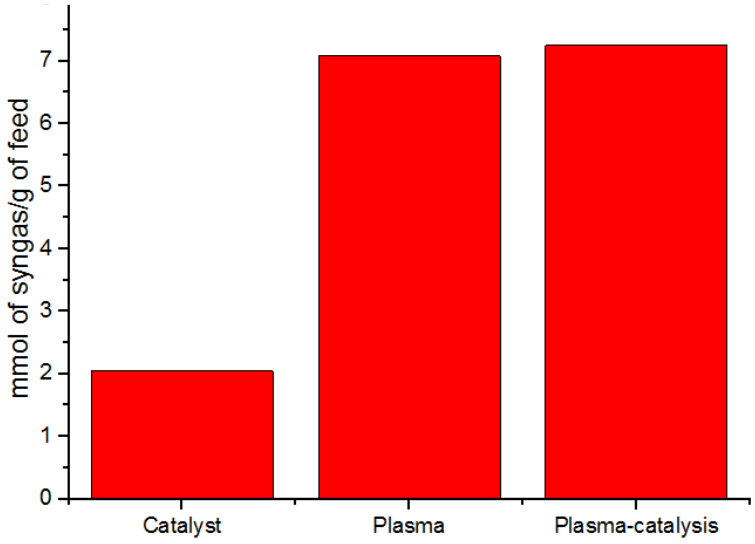

(b)

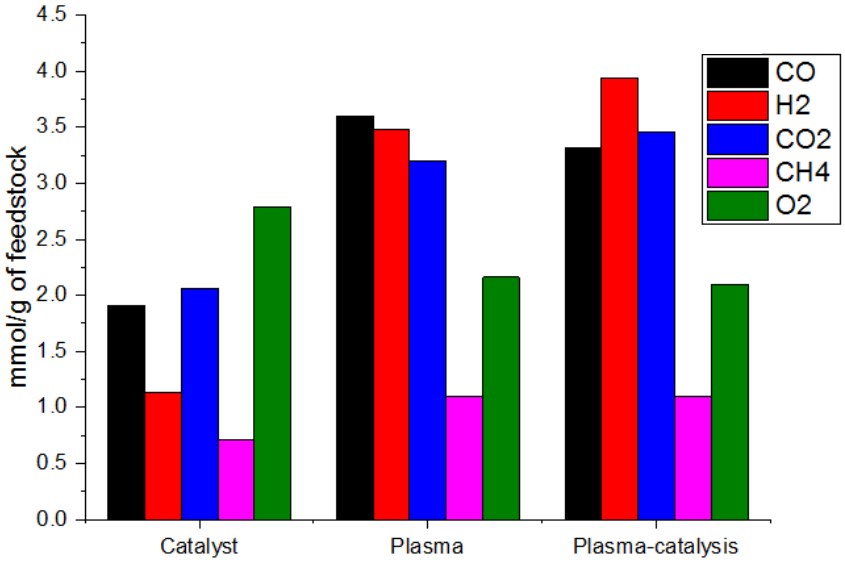

Fig.2. Comparison of 2(a) total syngas production and 2(b) detailed gas composition for catalysis, plasma and plasma-catalysis processes

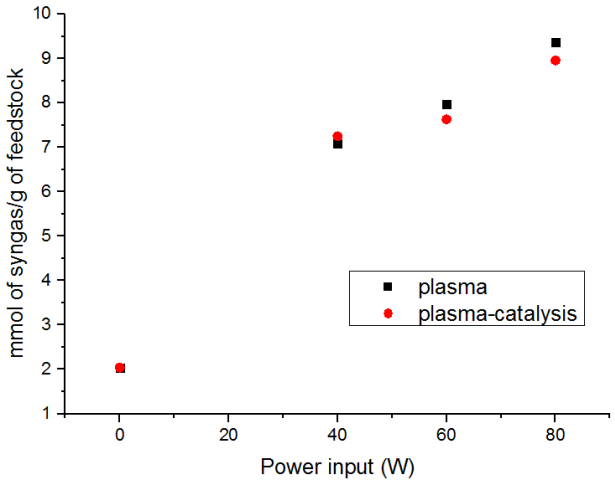

(a)

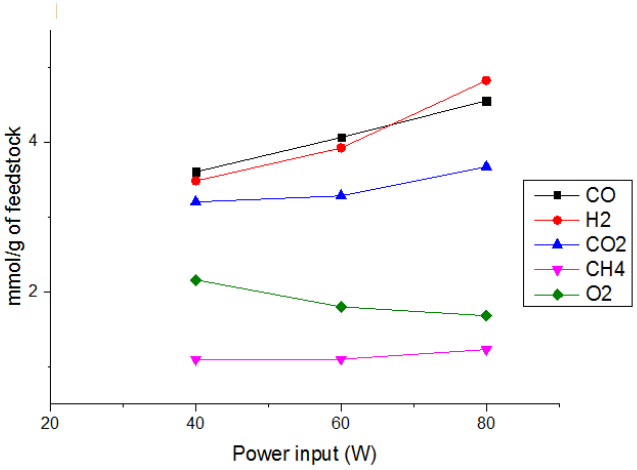

(b)

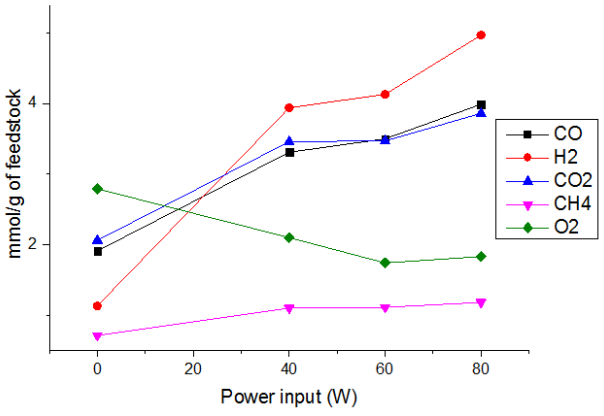

(c)

Fig.3. Comparison of 3(a) total syngas production and 3(b) detailed gas composition for plasma and 3(c) plasma-catalysis of biomass pyrolysis gases in relation to plasma input power

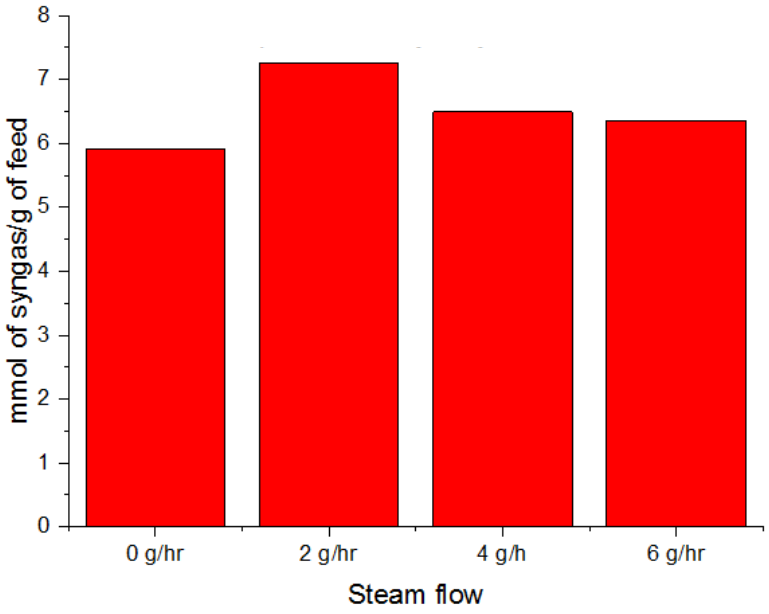

(a)

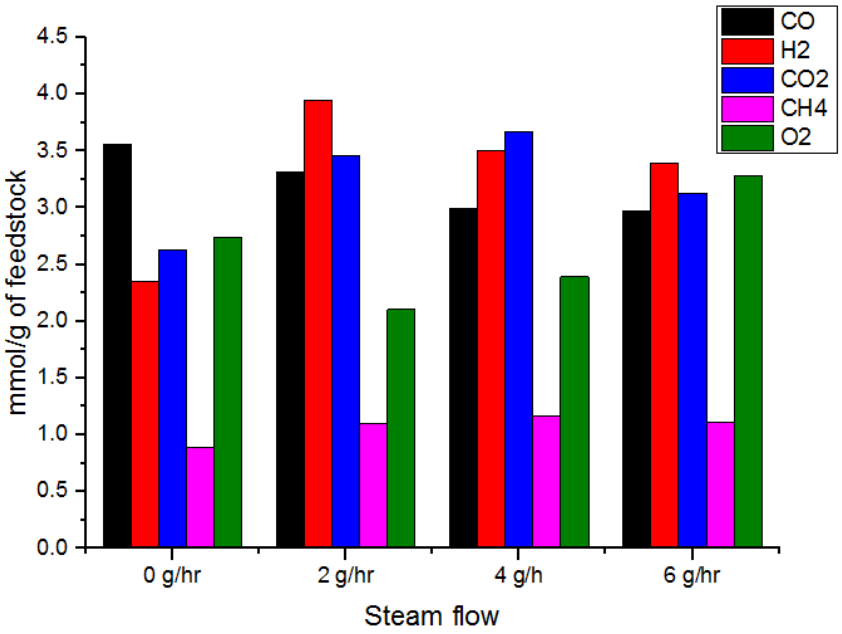

(b)

Fig. 4. Effect of steam flow on 4(a) syngas production and 4(b) detailed gas composition at 40 W input power for the pyrolysis-plasma-catalysis of biomass

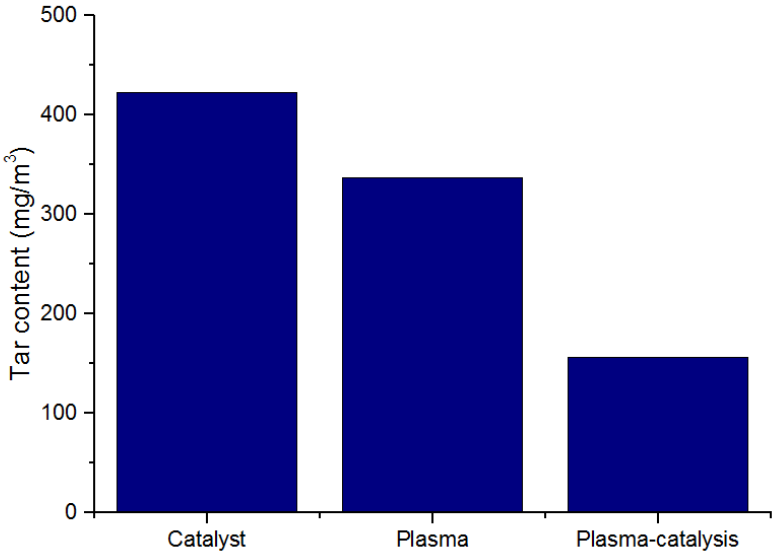

(a)

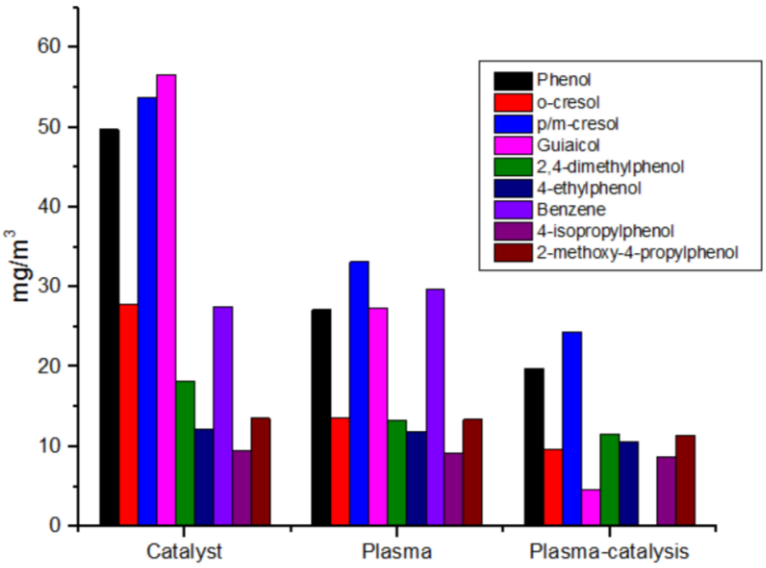

(b)

Fig. 5. Comparison of hydrocarbon tar content 5(a) and composition of selected tar compounds 5(b) for catalyst, plasma and plasma-catalysis of biomass pyrolysis gases.

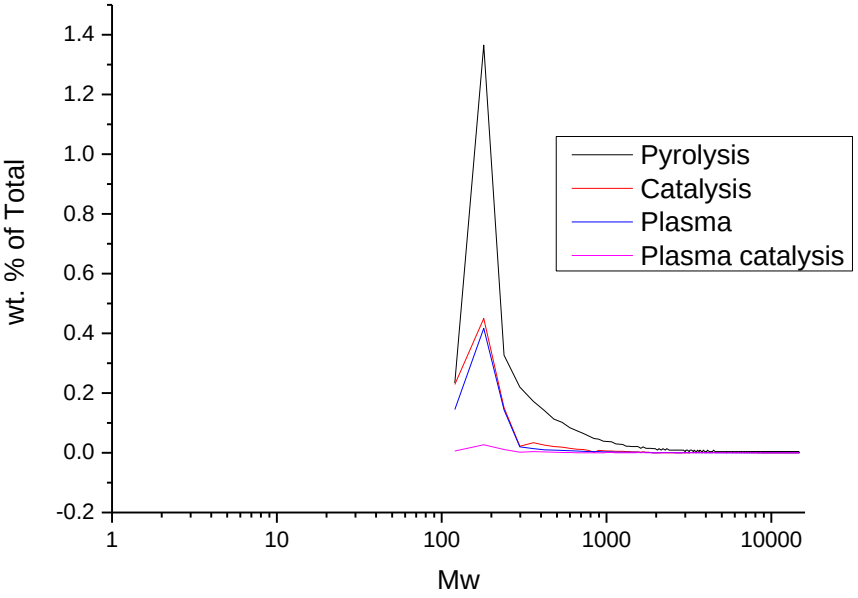

(a)

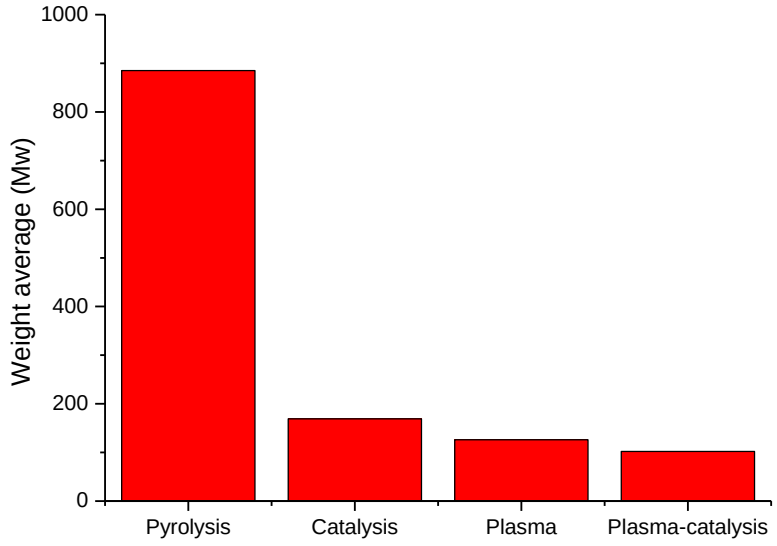

(b)

Fig. 6. Molecular weight range (6(a)) and the weight average molecular weight (6(b)) of the product condensed hydrocarbon tars.

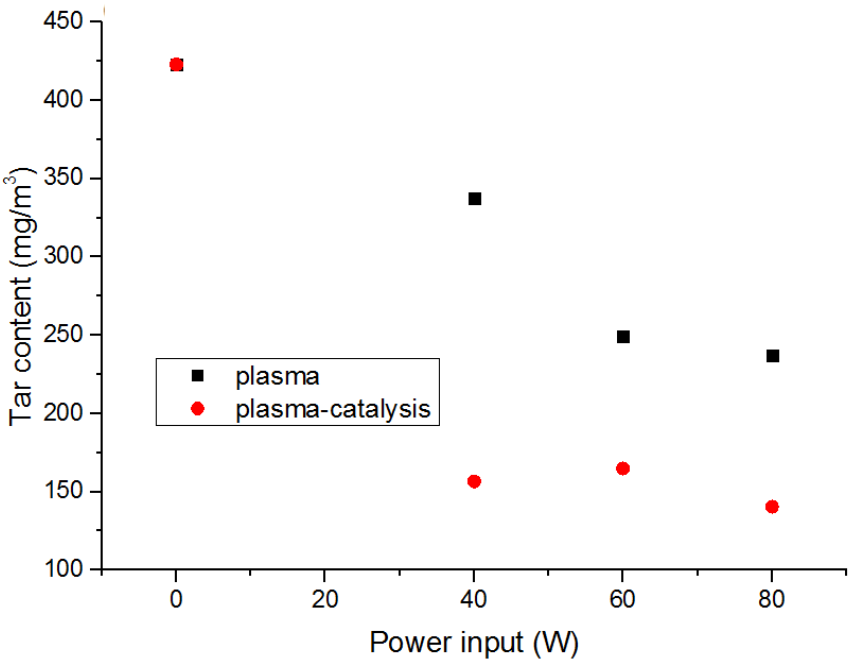

Fig. 7. Product gas tar content in relation to plasma input power, in relation to tar content for catalyst, plasma and plasma-catalysis of biomass pyrolysis gases

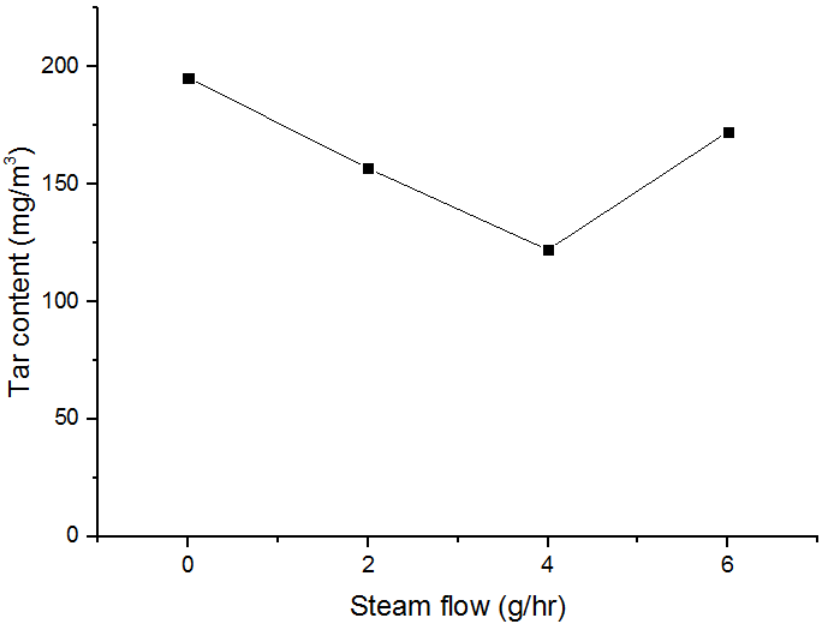

Fig. 8. Product gas tar content in relation to steam (water) input flowrate in relation to tar content for the plasma-catalysis of biomass pyrolysis gases

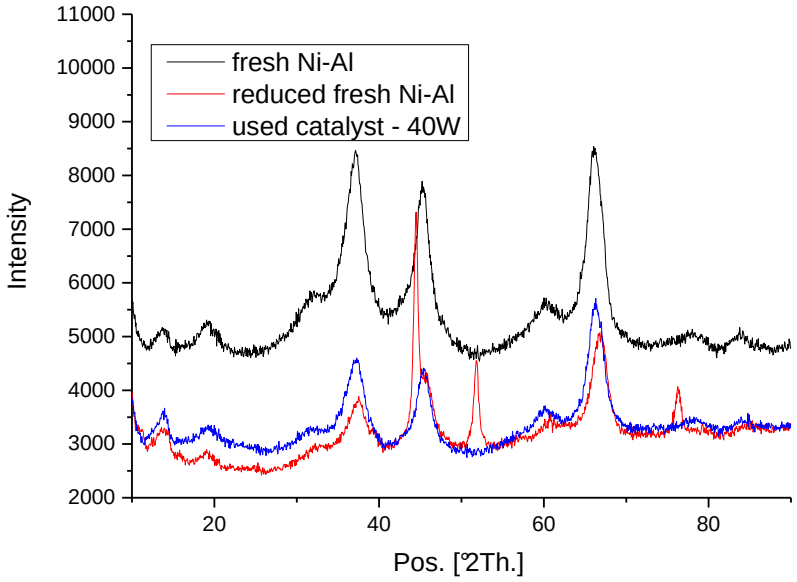

(a)

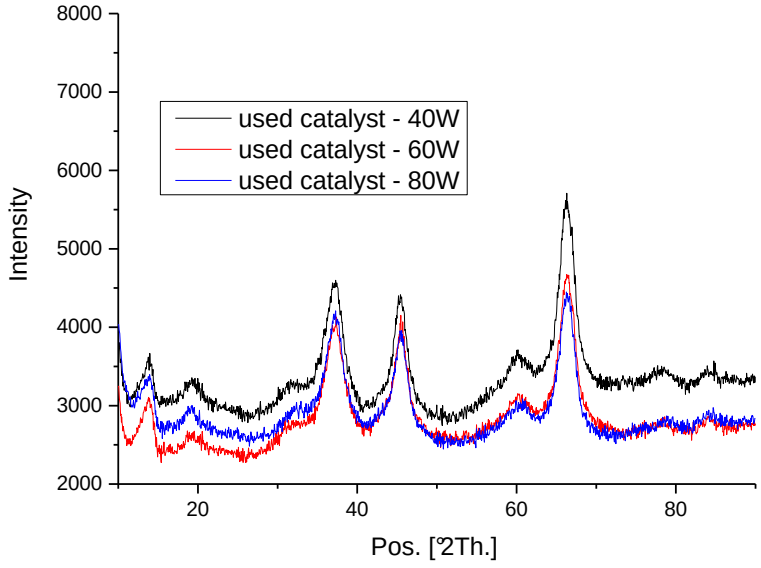

(b)

Fig. 9. XRD spectra of 9(a) the fresh, reduced and used plasma-catalysts and 9(b) the used plasma-catalysts in relation to power input